

Syntactic bulk metallic glass foam

A. H. Brothers and D. C. Dunand^{a)}

Department of Materials Science and Engineering, Northwestern University, Evanston, Illinois 60208

(Received 30 October 2003; accepted 17 December 2003)

An amorphous metal foam with a bulk density of 3.4 g/cm³ is created by low-pressure melt infiltration of the bulk metallic glass-forming alloy Zr₅₇Nb₅Cu_{15.4}Ni_{12.6}Al₁₀ into a bed of hollow carbon microspheres, followed by rapid quenching. The foam consists of a glassy metallic matrix containing ~60 vol. % of homogeneously distributed carbon microspheres, 25–50 μm in diameter, with small amounts of ZrC at the interface. An amorphous foam with 5 mm diameter showed no measurable loss in thermal stability as compared to the amorphous alloy in bulk form. © 2004 American Institute of Physics. [DOI: 10.1063/1.1646467]

Metallic foams are an emerging class of structural materials characterized by low density, high density-compensated mechanical properties, excellent mechanical energy absorption, and good acoustic dampening.¹ A variety of foaming processes exist, leading to a range of pore sizes and morphologies in open- and closed-cell architectures.² However, commercially developed metal foaming processes are not designed to accommodate the stringent purity and cooling-rate requirements of bulk metallic glass (BMG) alloys, which are necessary to prevent their crystallization during cooling.³

The motivation to adapt metal foaming processes to BMG requirements is foremost the potential for gains in macroscopic ductility through foaming. Monolithic BMG alloys, though very strong, fail by shear banding with almost no macroscopic plastic strain, limiting their usefulness as structural materials.³ However, extensive literature reviewed by Conner *et al.*⁴ has shown high bending ductility in a number of amorphous foils and wires (on the order of 10%–100% for Zr–Ti–Cu–Ni–Be alloys with dimensions below 1 mm), which was attributed to decreases in both shear band spacing and shear offset per band as sample dimension is reduced. Because the solid struts within foams are often less than 1 mm in size, and deform primarily by bending even when the foam itself is loaded uniaxially,¹ the struts of a BMG foam are expected to benefit from the same mechanism responsible for the high ductility of foils and fibers. Microscopic ductility in the struts should in turn translate into improved macroscopic ductility in the BMG foam.

Processing of BMG foams presents significant difficulties, however. First, introduction of pores during foaming leads to decreased thermal conductivity, which restricts the foam to dimensions smaller than those possible using a dense alloy. Moreover, the pore size of a BMG foam must be restricted to less than about 1/7 of this minimum foam dimension, if statistically reliable mechanical properties are sought.¹ Finally, only materials which do not induce heterogeneous nucleation in the BMG during cooling may be used during foaming, and only with appropriately low contact temperatures and times. This restriction is severe, as many foaming processes achieve the necessary high porosity and small feature size by incorporating a high volume fraction of

fine pore-forming materials (e.g., soluble placeholders, hollow spheres, gas-generating powders), which necessarily involves high contact area with the alloy.

A processing method for making BMG foams, taking into account these restrictions, was first proposed by Apfel and Qiu.⁵ They envisioned rapid cooling of a glass-forming melt containing an immiscible volatile liquid by pressure-quenching, during which the volatile liquid would vaporize explosively, taking its latent heat of evaporation from the remaining glass-forming melt. Though the method was investigated theoretically, no experimental confirmation was presented. San Marchi *et al.*⁶ achieved foam architectures with the glass-forming alloy Zr₅₇Nb₅Cu_{15.4}Ni_{12.6}Al₁₀ (Vit106) using various metal foaming methods, but did not attain amorphization due to contamination, which is particularly difficult to avoid in this alloy due to the high reactivity of Zr. Very recently, Schroers *et al.*⁷ reported the successful processing of a Pd₄₃Ni₁₀Cu₂₇P₂₀ BMG foam by melt-entrapment of water vapor released during the decomposition of a hydrated B₂O₃ flux. Because B₂O₃ is already used as a flux for reducing heterogeneous nucleation in Pd-based melts,⁸ this method is ideally suited to foaming of those alloys, which are among the best glass-formers known. It cannot, however, easily be extended to other BMG systems, in particular to the commercially relevant family of Zr-based BMG alloys. The high affinity of zirconium for hydrogen, oxygen, and boron would likely cause severe losses in glass-forming ability in these alloys. Oxygen, in particular, is known to be highly deleterious to Zr-based BMG even in low concentrations.^{9–11}

This letter describes an alternative BMG foam processing method that accommodates both the need for small BMG features, subjected to bending loads, and the need for a processing route generally applicable to contamination-prone Zr-based BMG alloys. The method is adapted from techniques used in the production of “syntactic” metal foams (foams whose low density is achieved by incorporating hollow particulates into the alloy) from Al¹² and Mg¹³ alloys.

Hollow carbon microspheres (Carbospheres, Inc., Fredericksburg, VA, with diameter 25–50 μm and wall thickness 1–10 μm) were suspended in acetone and centrifugally sedimented to separate intact from broken spheres. Intact spheres were cleaned ultrasonically in organic solvents and then

^{a)}Electronic mail: dunand@northwestern.edu

vacuum dried at the processing temperature (1250 K) for at least one hour to remove volatile components. A bed of dried spheres (~ 5 mm diameter and 8 mm height) was then placed into the sealed end of a stainless-steel tube (wall thickness < 1 mm), and a thin perforated graphite disk was placed above the bed to prevent premature contact between bed and melt. The tube was given a light coating of Y_2O_3 to minimize reaction with the melt and prevent dissolution of the carbon microspheres into the steel, and the whole crucible assembly was then preheated to 1250 K under high vacuum (3×10^{-5} Torr). After 30 minutes of equilibration, a pre-alloyed charge of $Zr_{57}Nb_5Cu_{12.6}Ni_{15.4}Al_{10}$ (base metals $\geq 99.5\%$ purity) was lowered into the hot zone and allowed to melt for 3 minutes and collect on top of the spacer disk. This melt was then infiltrated into the microsphere bed using 153 kPa of 99.9996% pure Ar gas. After a 45-second infiltration period, the infiltrated sample was quenched by immersion of the tube in a large bath of chilled and strongly agitated 8.5 wt. % NaCl brine solution. Infiltration was found to be uniform only in the lowest 3 mm at the bottom of the bed, and the material in that region was used for all tests described below. This part of the sample is believed to have cooled mostly radially, because the crucible bottom was more than 2.5 times thicker than its walls.

Figure 1(a) shows an optical micrograph of a Vit106 foam produced by this method. The figure demonstrates that the foam structure is uniform across the entire cross-section, with no evidence of sphere agglomeration, porosity due to poor wetting, or other macroscopic defects. Figure 1(b) shows a higher-magnification image of the same sample and highlights some of the features visible in the foam microstructure, which include irregularly shaped spheres, infiltrated spheres, and sphere fragments, found among a majority of hollow, uninfiltrated spheres. Infiltrated necks as narrow as $1 \mu m$ were found between particles, indicating excellent wetting, though occasional uninfiltrated necks were also present. Analysis of several hundred particles reveals that the proportion of broken and infiltrated spheres is $\sim 1\%$, and consequently these flaws only marginally impact overall density and properties; the proportion of misshapen spheres is much higher, $\sim 18\%$, with the remainder (81%) being roughly spherical and intact. Image analysis also shows that the volume fraction of Vit106 in the foam is 41%, with an estimated error of 2%. The net foam density, measured by helium pycnometry, is $3.4 \pm 0.2 \text{ g/cm}^3$, corresponding to a relative density ($\rho_{\text{foam}}/\rho_{\text{Vit106}}$) of $50 \pm 3\%$. This relative density is higher than the Vit106 volume fraction due to the additional mass of carbon. While the relative density is required for engineering design, the BMG fraction is expected to be more relevant to the mechanical properties of the foam, since the highly irregular thickness of the microsphere walls makes them unlikely to contribute appreciable strengthening.

Figure 2 shows x-ray diffraction data (using $Cu-K\alpha$ radiation) verifying the amorphous structure of the foam and demonstrating the presence of ZrC, which was not visible using either optical or scanning electron microscopy. Submicron interfacial ZrC has been observed in studies of similar Zr-based alloys with carbon fibers and carbide particulates,^{14,15} where it was concluded that the formation of ZrC does not significantly affect the glass-forming ability of the

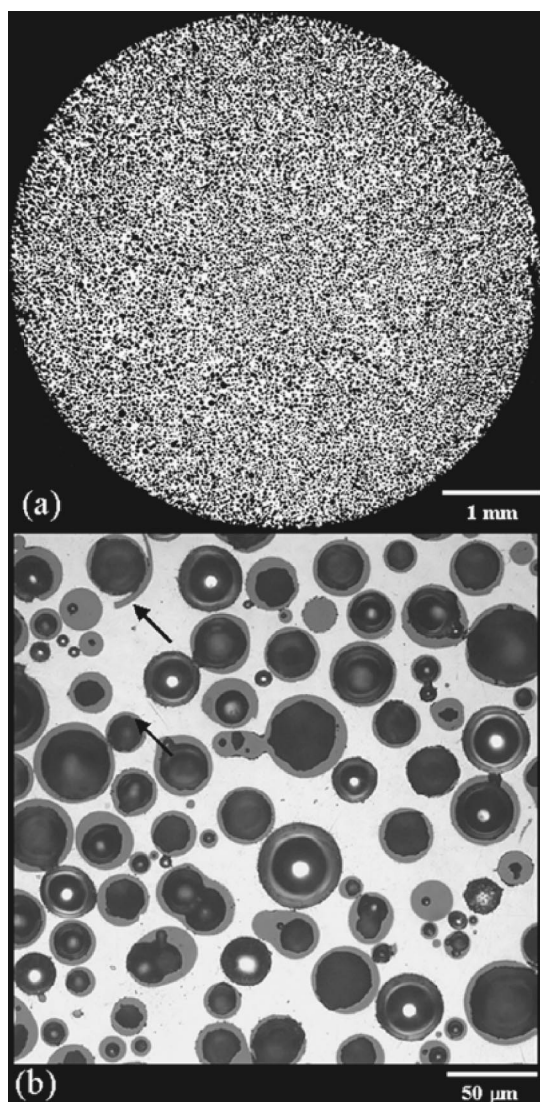


FIG. 1. Optical micrographs showing the structure of syntactic Vit106 foam: (a) Low magnification image demonstrating foam uniformity; (b) magnified image of the surface showing microscopic foam structure. Misshapen carbon microspheres are visible, as is a sphere wall fragment (indicated by arrow). Good wetting is inferred from the lack of interparticle porosity.

host alloys. In a separate study,¹⁶ it was shown that interfacial ZrC allows for the reactive wetting of the BMG alloy $Zr_{41.2}Ti_{13.8}Cu_{12.5}Ni_{10.0}Be_{22.5}$ (Vit1) onto carbon substrates above 1200 K. The present low-pressure infiltration of a viscous Vit106 melt around small carbon microspheres likely

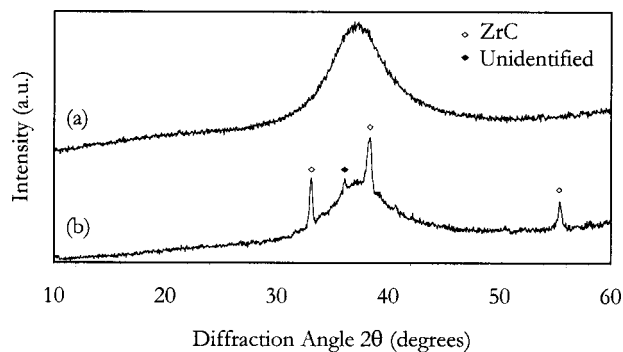


FIG. 2. X-ray diffraction patterns collected from: (a) Fully dense amorphous Vit106; (b) the surface of the Vit106 foam shown in Fig. 1(a). Crystalline reflections are indicated by markers.

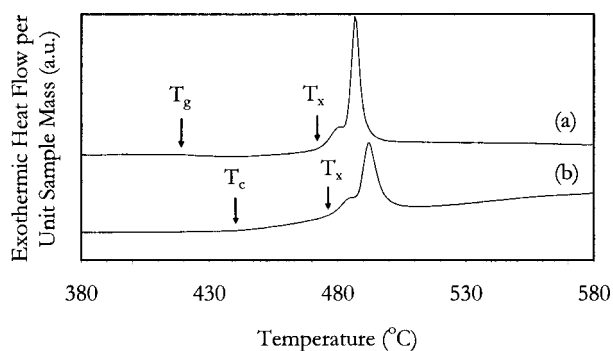


FIG. 3. DSC thermograms indicating glass transition temperatures T_g and onset temperatures of crystallization T_x for: (a) Fully dense amorphous Vit106 from the sample analyzed in Fig. 2(a); (b) Vit106 foam from Figs. 1 and 2(b).

relies on the reactive wetting resulting from the presence of ZrC. A much less pronounced peak is also visible in Fig. 2(b), which does not correspond to ZrC. This peak corresponds to a major reflection of Nb₂C, which is only slightly less stable than ZrC and may, therefore, have formed in small amounts; however its small size and lack of higher-order reflections prevent conclusive identification.

Results of differential scanning calorimetry (DSC), performed with a heating rate 0.33 K/s under argon on a small section of foam and an amorphous Vit106 sample taken from the same ingot used to make this foam, are shown in Fig. 3. The thermogram for dense Vit106 exhibits a glass transition endotherm (onset at T_g) and two-stage crystallization exotherm (onset at T_x) appearing at 418 °C and 473 °C, respectively (all transition temperatures are estimated by the standard method of linear intercepts). These values are close to ones reported elsewhere for bulk Vit106.¹⁵ The Vit106 foam shows the same two-stage crystallization behavior as the unprocessed Vit106, at nearly the same temperature ($T_x = 477$ °C). The heat of crystallization of the dense alloy is estimated at 48 J/g, which matches within 15% that of the foam after adjusting for its lower Vit106 content (54 J/g). From these facts, it is concluded that the fundamental crystallization pathway of the Vit106 matrix is unchanged in the presence of carbon microspheres and that the foam is processable as a supercooled liquid at temperatures below ~473 °C, similar to bulk Vit106.

The BMG foam glass transition, however, is obscured by a slow exothermic feature beginning near 440 °C [T_c in Fig. 3(b)] and continuing past the end of the scan. It is unlikely that this feature reflects decomposition or crystallization of the glassy matrix, since the position and shape of the later exotherms (some 35 °C higher) are the same as those of the dense alloy. Rather it probably represents growth of the pre-existing ZrC at the microsphere interface. Using handbook values of the standard heat of formation of ZrC¹⁷ and the heat capacity of Zr, C, and ZrC,^{17,18} it is calculated that the conversion of all the Zr in the DSC sample into ZrC (at a characteristic temperature of 500 °C) would release ~10 J of heat. The integrated area of the background feature, up to a temperature of 580 °C, is about 1.4 J, such that carburization

of less than 15% of the Zr in the alloy would be sufficient to explain the feature. The feature area appearing prior to the onset of crystallization is <0.1 J, so that <1% of the Zr in the sample (beyond the amount reacted during processing) would have reacted during the DSC test prior to crystallization; this explains how the crystallization process and thermal stability may be unchanged despite the formation of ZrC, and the attendant loss of Zr from the matrix, during the scan.

In summary, a method has been developed to produce a closed-cell, amorphous Vit106 foam by low-pressure infiltration of carbon microspheres; the resulting foam exhibits a bulk density of ~3.4 g/cm³ with no measurable loss in stability. This method should apply to any BMG alloy which reactively wets microspheres at high temperature without contamination or nucleation inducing crystallization. Use of BMG alloys in foam architectures, where loads are carried mostly in bending by small strut sections, is expected to lead to marked improvements in macroscopic ductility relative to monolithic glass. It is also anticipated that these foams will show additional properties common to other metallic foams, including high density-compensated mechanical properties, mechanical energy absorption, and acoustic damping.

The authors acknowledge the support of DARPA's Structural Amorphous Metals program and of the Caltech Center for Structural Amorphous Metals. They also thank Professor J. H. Perepezko for producing the bulk Vit106 ingots, and Dr. D. K. Balch for preliminary experiments.

- ¹M. F. Ashby, A. Evans, N. A. Fleck, L. J. Gibson, J. W. Hutchinson, and H. N. G. Wadley, *Metal Foams: A Design Guide* (Butterworth-Heinemann, Boston, 2000).
- ²J. Banhart, *JOM* **52**, 22 (2000).
- ³J. E. Löffler, *Intermetallics* **11**, 529 (2003).
- ⁴R. D. Conner, W. L. Johnson, N. E. Paton, and W. D. Nix, *J. Appl. Phys.* **94**, 904 (2003).
- ⁵R. E. Apfel and N. Qiu, *J. Mater. Res.* **11**, 2916 (1996).
- ⁶C. San Marchi, A. Brothers, and D. C. Dunand, *Mater. Res. Soc. Symp. Proc.* **754**, CC1.8.1 (2003).
- ⁷J. Schroers, C. Veazey, and W. L. Johnson, *Appl. Phys. Lett.* **82**, 370 (2003).
- ⁸N. Nobuyuki and A. Inoue, *Mater. Trans., JIM* **38**, 464 (1997).
- ⁹M. F. de Oliveira, W. J. Botta F., M. J. Kaufman, and C. S. Kiminami, *J. Non-Cryst. Solids* **304**, 51 (2002).
- ¹⁰X. H. Lin, W. L. Johnson, and W. K. Rhim, *Mater. Trans., JIM* **38**, 473 (1997).
- ¹¹A. A. Kündig, D. Lepori, A. J. Perry, S. Rossmann, A. Blatter, A. Dommann, and P. J. Uggowitzer, *Mater. Trans., JIM* **43**, 3206 (2002).
- ¹²P. K. Rohatgi, R. Q. Guo, H. Iksan, E. J. Borchelt, and R. Asthana, *Mater. Sci. Eng., A* **244**, 22 (1998).
- ¹³J. Sugishita, S. Fujiyoshi, T. Imura, and M. Ishii, *Wear* **81**, 209 (1982).
- ¹⁴C. P. Kim, R. Busch, A. Masuhr, H. Choi-Yim, and W. L. Johnson, *Appl. Phys. Lett.* **79**, 1456 (2001).
- ¹⁵H. Choi-Yim, R. Busch, U. Köster, and W. L. Johnson, *Acta Mater.* **47**, 2455 (1999).
- ¹⁶J. Schroers, K. Samwer, F. Szuets, and W. L. Johnson, *J. Mater. Res.* **15**, 1617 (2000).
- ¹⁷O. Kubaschewski and C. B. Alcock, *Metallurgical Thermochemistry*, 5th ed. (Pergamon, New York, 1979).
- ¹⁸*Thermochemical Properties of Inorganic Substances II*, 2nd ed., edited by O. Knacke, O. Kubaschewski, and K. Hesselmann (Springer, New York, 1991).